Potential-Induced Degradation (PID): Introduction of a Novel Test Approach and Explanation of Increased Depletion Region Recombination

Dominik Lausch, Volker Naumann, Otwin Breitenstein, Jan Bauer, Andreas Graff, Jöerg Bagdahn, and Christian Hagendorf

***Abstract*—In recent years, a detrimental degradation mechanism of solar cells in large photovoltaic fields called potential-induced degradation (PID) has been intensively investigated and discussed. Here, the module efficiency is decreasing down to a fractional part of their original efficiency. In this study, we introduce a PID test at a solar-cell level and for individual module components applicable as a tool for process control in industries and root cause analyses in science departments. Using the proposed method, one example analysis of a solar cell that is degraded by the PID tester is presented. It is shown that PID of the shunting type influences both the parallel resistance (R_p) and the depletion region recombination behavior (J_{02}) of the solar cell. Increased recombination in the depletion region is caused by Na decorated stacking faults crossing the depletion region. This strongly influences recombination behavior in the depletion region, leading to an increased J_{02} and an ideality factor $n_2 > 2$. However, the defects leave the base of the solar cell primarily unaffected, and hence, J_{01} recombination remains rather low. Based on these findings, a model for the shunting and the increased depletion region recombination behavior is discussed.**

***Index Terms*—Crystal defect, potential-induced degradation (PID), recombination.**

I. Introduction

ONE of the most important advantages of photovoltaic (PV) technology is its low cost of maintenance and a lifetime of over 30 years. Nevertheless, several degradation mechanisms can decrease solar efficiencies or destroy PV modules. Potential-induced degradation (PID) of crystalline Si solar cells is one of the main degradation mechanisms and has been intensively investigated since the affect was reported more than two years ago [1], [2]. This effect has been most pronounced in large field installations of PV modules that are fabricated using p-type solar cells. In conventional PV systems under working conditions, a voltage difference of a few hundred volts between the framing and the solar cells of a module can occur. If the modules/cells are not resistant to PID, the degradation mechanism can result in yield losses of 20% or more. According to recent publications, the PID shunting effect (PID-s) is the most relevant type of PID [3]–[5]. However, it has also been shown that PID-s can also influence the recombination behavior of the solar cell [3], [6]. In this paper, it is shown that these recombination processes mainly influence the second diode (J_{02}) that is caused by increased recombination in the depletion region because of Na-decorated stacking faults.

To prevent PID in the field, either every solar cell in the module, or module components such as encapsulants or glass must be PID resistant. For PID testing, various methods exist at module and solar-cell level. Generally, PID susceptibility is tested in a climate chamber [7] (damp heat, 85 °C, 85% relative humidity, −1000 V, 48-h test time) or in a water bath on the module level [1]. However, for such tests, a module or minimodule must be prepared, and a climate chamber is necessary.

At the cell level, to prevent PID, the solar cell must be resistant to PID-s. One way to achieve this is to optimize the antireflection coating (ARC). However, in a module every solar cell has to be resistant to PID. To test resistance to PID-s, a quick and direct process control method is required. To test PID susceptibility on a solar-cell level, a high-voltage stress test by corona discharge can be used [4], [8]. Here, a voltage stress of around 20 keV is used. However, single-module components, i.e., encapsulants and glass, cannot be tested using this method. In addition, only single positions to where the cathode is pointing can be tested for PID susceptibility. The high-voltage stress can also lead to a transformation of the SiN, often leading to a visible permanent discoloration on the SiN layer. Repeatability using this method is also difficult since the charging is dependent on climatic factors such as humidity and temperature. Hence, the corona PID test needs well-defined environmental conditions. For an alternative method, a test was proposed in which the solar cell is connected by tab ribbons, with glass-EVA laminates on both sides. Subsequently, the whole sample is then placed in a climate chamber to perform the PID test. However, it was concluded that this method did not work, and laminated minimodules were again produced [7].

Manuscript received June 10, 2013; revised July 26, 2013, November 12, 2013, and December 9, 2013; accepted December 10, 2013. Date of publication March 27, 2014; date of current version April 18, 2014.

D. Lausch, V. Naumann J. Bagdahn, and C. Hagendorf are with the Fraunhofer Center for Silicon Photvoltaics CSP, D-06120 Halle (Saale), Germany (e-mail: dominik.lausch@csp.fraunhofer.de; volker.naumann@csp.fraunhofer.de; joerg.bagdahn@csp.fraunhofer.de; christian.hagendorf@csp.fraunhofer.de).

O. Breitenstein and J. Bauer are with the Max Planck Institute of Microstructure Physics, 06120 Halle, Germany (e-mail: breiten@mpi-halle.mpg.de; jbauer@mpi-halle.mpg.de).

A. Graff is with the Fraunhofer Institute for Mechanics of Materials IWM, Walter-Hülse-Str. 1, 06120 Halle (Saale), Germany (e-mail: a.graff@iwmh.fraunhofer.de).

Color versions of one or more of the figures in this paper are available online at http://ieeexplore.ieee.org.

Digital Object Identifier 10.1109/JPHOTOV.2014.2300238

In this paper, a method to test the resistance against PID on the solar-cell level close to field conditions is introduced in Section III it is capable of testing individual solar cells as well as individual module components. Subsequently, a root cause analysis of a solar cell that is degraded by the PID tester is shown in Section IV, highlighting the influence of PID-s on the shunting and recombination behavior of the solar cell. In order to discuss the increased recombination behavior, a root cause analysis down to the nanometer scale is shown in Section V. Finally, a discussion about a model recently introduced [5] explaining the influence of PID-s on shunting and recombination behavior of the solar cell is presented in Section VI.

II. Experimental Details

The solar cells that are analyzed in this study are full-square monocrystalline silicon (mono-Si) solar cells produced in a commercial environment. The solar cells were degraded by the PID tester as it will be described in Section III. Electroluminescence (EL) images have been acquired with a coolSamBa HR-830 Si camera. The dark lock-in thermography (DLIT) measurements were performed with equipment from Thermosensorik, which offers the opportunity to increase the lateral resolution by different lenses. For more information, see [9]. The scanning electron microscopy (SEM) and electron-beam-induced current (EBIC) were acquired with a SU-70 (Hitachi) tool that is equipped with an EBIC system DISS 5 by point electronic. The electron beam energy for SEM and EBIC was varied between 3 and 30 keV.

Chemical information was measured by time-of-flight secondary ion mass spectroscopy (ToF-SIMS) within a TOF.SIMS 5 by IONTOF with a pulsed Bi primary ion beam scanning over the sample surface. ToF-SIMS depth profiling uses an additional O^{2+} (1 keV) sputter beam for planar erosion of surficial layers. Cross sections have been prepared by focused ion beam (FIB) and imaged by SEM/EBIC. Cross-sectional lamellae have been imaged by scanning transmission electron microscopy (STEM) in FEI TITAN^3 G2 60-300 equipped with spherical aberration correction and a Super-X EDX detector.

III. Introduction of a Novel Test Approach

An experimental setup for PID testing at solar-cell level was developed in order to provide a quick and easy tool for research and process control. With this setup, it is also possible to test partially fabricated solar cells such as wafers with ARC coating. Furthermore, individual module components such as special glasses or alternative foils as encapsulants can be tested as well. This opens the opportunity to test materials and solar cells before an application into the production processes. Here, a few test samples out of the production shall be tested in regular time steps for process control. Additionally, based on a special foil treatment, the solar cell can easily be delaminated without leaving residual contaminations on the solar-cell surface, hence, giving the possibility of performing advanced root cause analysis.

The prototype of the PID tester is shown in Fig. 1. The PID test is performed as follows: The solar cell is placed on a temperature-controlled aluminum chuck to achieve a constant

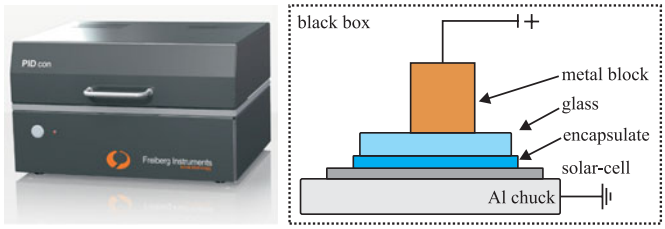

Fig. 1. (Left) PID tester by Freiberg Instruments. (Right) Simplified sketch of the specimen stacking which is similar to the structure of PV modules is visualized.

temperature throughout the testing process. On the front side, a layer of foil and a sheet of glass are placed on top of the solar cell. The specimen stack is shown schematically on the right side of Fig. 1. The stack can be made with all possible materials, but in this paper, only standard materials are used. To measure the solar-cell parameters, electrical contact to the front surface of the solar cell is realized by a contact needle (which is located outside the test region) and electrical contact at the rear is realized by the aluminum chuck. A solid metal block is then placed on top of the front glass to achieve a uniform high voltage across the glass surface within the test area. The test can be performed on samples with or without laminating the foil to the solar cell. Without the lamination process, it is possible to detach the foil after testing and allow for further investigations. A voltage of up to 1000 V is then applied. Under field conditions, the frame and subsequently the glass are grounded, leaving the solar cell at a negative potential. As only the potential difference is important for PID, in our test a positive voltage is applied to the solid metal block, and therefore, the glass surface and ground to the rear contact of the solar cell through the aluminum chuck. During the degradation, the shunt resistance, the *I–V* curve of the solar cells, and the HV ionic/leakage current can be measured. For our tests, we do not laminate the foil to allow for further investigations. Since the specimen stack approximates the module structure, standard module materials are used. We also use a voltage of 600 V and temperature of 80 °C, similar to that which occur under field operation. Therefore, we assume that test procedure is performed under realistic conditions close to what is experienced in the field, and hence, the results should be trustworthy. However, a conductive layer on top of the solar glass at temperatures of about 80 °C can be doubted since the wet glass surface will dry quickly under real conditions, although the electric field will be still present at the frame. Nevertheless, the method will still be close to standard test conditions. If the standard test conditions for PID are different from those used in this study, then the test procedure can be easily adapted to more appropriate conditions. In addition, all comparisons between our tester and module tests in climate chambers have shown equal results.

In order to test alternative encapsulants and glasses, a PID-prone solar cell has to be used for the PID test. If the solar cell is not PID affected, the encapsulants and glasses, respectively, are preventing PID.

In Fig. 2(a), a dark *I–V* curve is shown as an example measurement of a solar cell before (black) and after (red) the PID

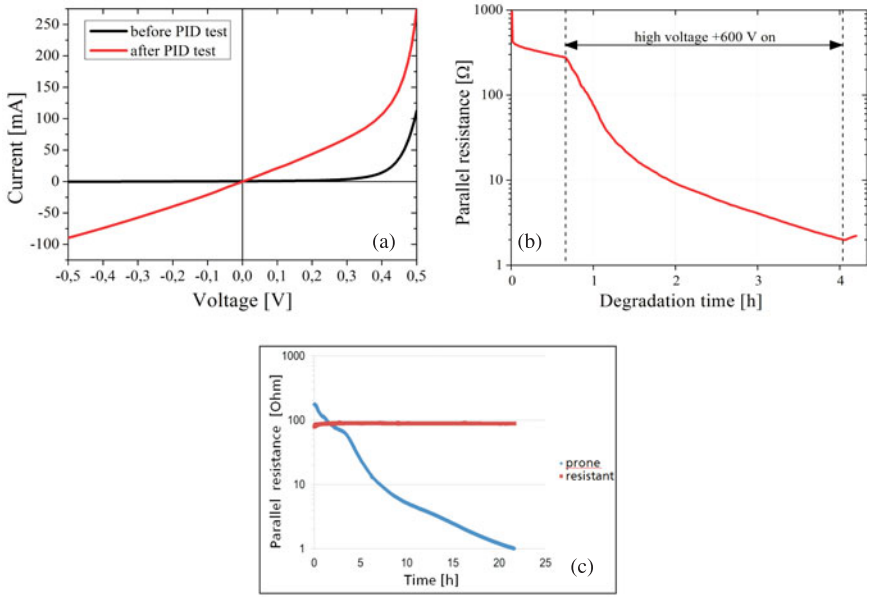

Fig. 2. (a) Dark *I–V* curve of a solar cell before (black) and after (red) PID test of a 4 × 4 cm^2 area at 600 V, (b) degradation of the parallel resistance of a tested solar cell, and (c) parallel resistance throughout the test for a solar cell with an encapsulant prone to and resistant to PID.

test of a 4 × 4 cm^2 area at 600 V. A distinct ohmic behavior of the solar cell is indicated by the linear *I–V* characteristic around $U = 0$ V. However, the slightly curved shape of the *I–V* curve for higher voltage indicates the presence of an additional nonlinear current component. The parallel resistance R_p was measured every 30 s during the whole test by applying a voltage $U = -0.1$ V at the solar cell for the duration of each measurement. The time dependence of the degradation is shown in Fig. 2(b). During the test, R_p decreases until the voltage is turned OFF. This indicates PID-s degradation of the solar cell by the PID tester, as has been shown from field experiments by Taubitz *et al.* [6]. In Fig. 2(c), a PID test of the same solar cell with a PID resistant and a PID-prone encapsulant is shown. The R_p of the solar cell that is tested with the PID resistant encapsulant is nearly constant over the whole test duration, proving that the encapsulant is preventing PID, whereas the R_p decreases when using a PID-prone encapsulant. This result is further supported by tests at the module level.

Since the introduced method uses the same material stack as well as the same materials for the stack as used for modules, and the voltage and temperature is as occurring under field operation (of up to 1000 V and 90 °C), it can be assumed that the introduced procedure is testing on PID susceptibility of solar cells or module components rather than other degradation mechanisms, as could be the case for different test procedures.

IV. Characteristics of Potential-Induced Degradation-s on the Solar-Cell Level

As can be seen in Fig. 2(b) and (c), respectively, R_p is strongly decreased after PID, as shown in [1]. In addition to this, Taubitz *et al.* [6] and Hacke *et al.* [3] have shown that the illuminated *I–V* characteristic cannot be fitted by a decreased R_p alone. It was shown that a second diode must be added in order to fit the illuminated *I–V* curve correctly. We assume that this is because of an increased recombination process at PID-s-affected positions. If this is the case, the recombination takes place in the depletion region. This assumption will become clear throughout this paper. This would result in an increased J_{02} and high ideality factor $n_2 > 2$ and will be discussed later.

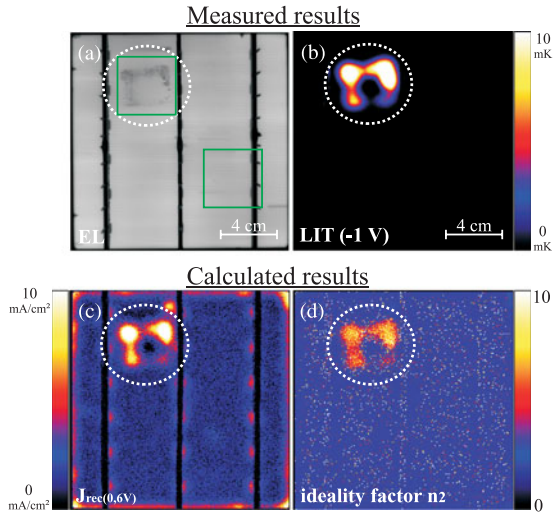

Fig. 3. (a) EL image of a degraded solar cell (measured). The green marked regions have been taken out for dark *I–V* measurements. (b) DLIT image at −1 V. The shunted region is revealed by the increased DLIT signal (measured). (c) J_{02} distribution calculated from four DLIT measurements at different voltages according to [11] (calculated). (d) Ideality factor n_2 (calculated), scaled from 2 to 10. The PID-s region exhibits a strongly increased J_{02} and an ideality factor n_2 up to 7.

In Fig. 3(a), an EL image of a PID-s-degraded full-square mono-Si solar cell is shown. The solar cell was PID-s degraded on a 4 × 4 cm^2 area, which is characterized by a strongly decreased EL signal between the busbars [marked by a white

circle in Fig. 3(a)]. In Fig. 3(b), a DLIT image of the same solar cell at -1 V is shown. The DLIT image reveals that strong shunts in the PID-s-affected area are in good agreement with previous results [10]. As already discussed, PID-s degradation results in a strong local decrease of R_p.

Based on a procedure introduced by Breitenstein [11], it is possible to calculate the local *I–V* curves out of four different DLIT measurements. In addition, the parameters of the two-diode model of each pixel can be imaged, including the ideality factor n_2 of the depletion region recombination current. For this, we have performed DLIT analyses at -1 V, 500, 550, and 600 mV. J_{01} shows a rather even distribution over the whole solar cell (not shown here). Small deviations at the contacts can be observed. These deviations could be caused by a laterally varying serial resistance (R_S). In our calculations, R_S is assumed to be constant. In contrast with this, J_{02} is strongly increased at the degraded area, which can be seen in Fig. 3(c). Based on these results, it is assumed that at PID-s-affected sites, a strong recombination process in the depletion region takes place since J_{02} is influenced by recombination processes within the depletion region. An increased J_{02} can also be observed at the corners of the solar cell. This can be expected if the p-n junction is opened poorly there, having a large number of defects [12]. In Fig. 3(d), the calculated ideality factor n_2 is shown. Fig. 3(d) shows that the ideality factor in severely PID-s-affected areas reaches local values of up to 7.

Strongly increased J_{02} values and ideality factors larger than 2 for PID-s-affected areas can also be observed in multicrystalline Si (multi-Si) solar cells. In contrast with mono-Si, the increased J_{02} in multi-Si solar cells is subjected to recombination-active defect structures, in particular so-called type-A defects [13], which can also result in an increased J_{02}. However, J_{02} for PID-s-affected areas is much higher than that caused by recombination-active defects.

In order to confirm the DLIT results, we have taken two regions out of the degraded solar cell as marked with the green rectangles in Fig. 3(a). In Fig. 4, the dark *I–V* characteristics of these regions (a PID affected and a reference region) are shown. To discuss the solar-cell parameters, we have fitted the curves with the two-diode model. The parallel resistance of the PID-affected region is about 500 $\Omega{\cdot}\text{cm}^2$ which is drastically reduced compared with 33 $\text{k}\Omega{\cdot}\text{cm}^2$ of the reference position. The recombination current J_{02} of the PID-affected region is about $5\times10^{-16}\,\text{A/cm}^2$ and, hence, clearly higher compared with the reference region $(1\times10^{-19}\,\text{A/cm}^2)$. The J_{01} currents are quite similar. The calculated ideality factor n_2 of the whole PID-affected region is approximately $n_2 = 3.2$: lower than that determined by the DLIT analysis. However, the n_2 value of the *I–V* curve is the mean value of the whole region and therefore, includes regions which are not degraded. Hence, the *I–V* curve analysis confirms the DLIT measurements.

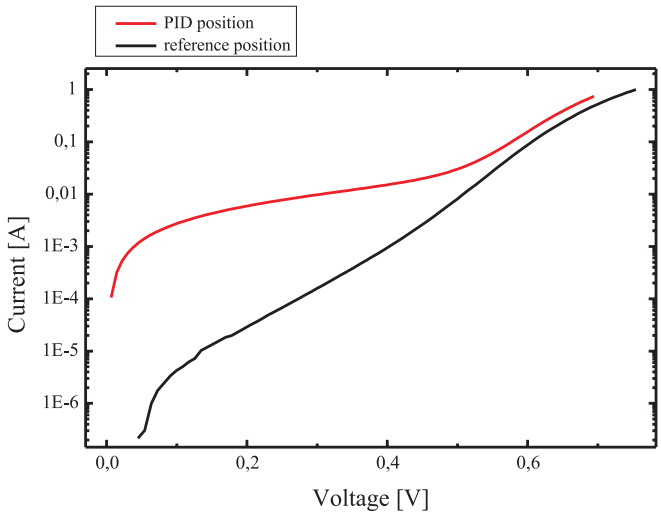

Fig. 4. Dark *I–V* curve of the two samples which were taken out of the degraded solar cell [marked in Fig. 3(a) with a green rectangle].

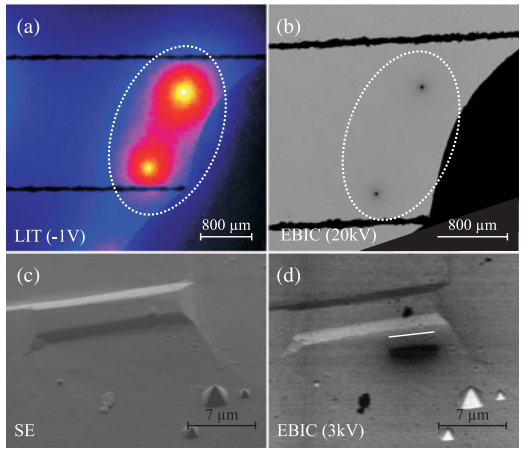

Fig. 5. (a) DLIT image at high magnification of two PID-s positions. (b) EBIC (20 kV) of the same region. The PID-s positions can be seen as reduced EBIC signal. (c) SE image at 3 kV of a PID-s position. No evidence as root cause for PID-s can be seen. (d) EBIC image at 3 kV. Here, PID-s is characterized by a line-shaped reduced EBIC signal.

V. Microscopic Investigation of Potential-Induced Degradation

In Fig. 5(a), a DLIT image at -1 V and high magnification can be seen. Two PID-s positions marked with a white-dotted circle between two contact fingers have been obtained. The EBIC signal at these positions is drastically reduced, as seen in the EBIC image in Fig. 5(b) (20-kV acceleration voltage). In general, the PID-s-affected areas are very localized, as shown in [10]. In Fig. 5(c) and (d), a PID-s-affected area is investigated by SE imaging (c) and EBIC (d) in high magnification and with a lower acceleration voltage 3 kV. Here, two important facts should be emphasized: 1) The SE image in Fig. 5(c) shows no particular feature visible at the surface except small pyramids and the edges of truncated pyramids since the mono-Si solar cell is weakly alkaline textured [14]. 2) The EBIC signal in Fig. 5(d) is reduced and visualized by the white line. The line is approximately 4 μm long and parallel to the pyramidal structures; hence, the long axis of PID-s-affected areas appears to be oriented along a $\langle 1\ 1\ 0\rangle$ direction. The fact that the line has one sharp and one smooth edge indicates that the corresponding defect is lying inclined to the (1 0 0) surface [15] because at this

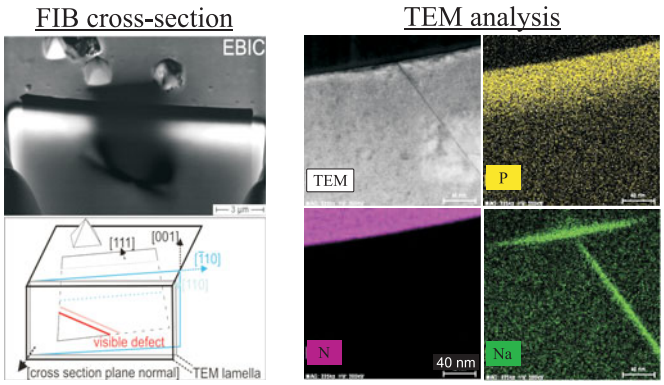

Fig. 6. (Left) Cross-sectional EBIC view of a shunt position. A disturbed p-n junction and a distinct linear region with low signal both in cross section and on the surface can be seen. The scheme is visualizing the geometrical position of the crystal defect (taken from [15]). (Right) STEM analysis of a FIB-lamella showing a PID-s degraded stacking fault that hits the Si surface. The elemental intensities were measured by EDX in STEM mode (taken from [16]).

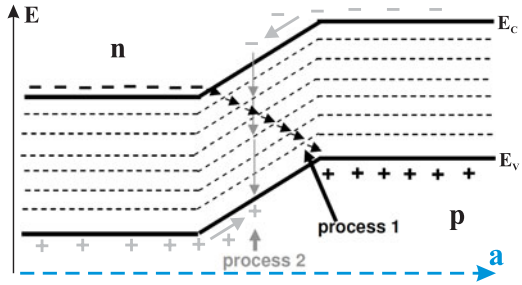

Fig. 7. Band structure along a Na decorated stacking fault [5]. The defect states are illustrated with dotted lines. For sufficiently high concentration levels of Na, hopping conduction of carriers can occur via the introduced defect levels (process 1). For lower concentration levels, electrons and holes can recombine via these defect levels under forward bias in the depletion region, leading to an increased J_{02} and n_2 (process 2). Here, the carriers are generated by illumination.

surface, electrons have a high collection probability, and the interaction volume with the electron beam is small, resulting in a high lateral resolution. Within the silicon material, the signal is blurred because of carrier diffusion and the collection probability of carriers which are generated near the defect. The same behavior has been observed at over 30 different PID-s-affected areas of different samples, even on multi-Si solar cells. It should be noted that in multi-Si solar cells PID-s-affected areas are not located at grain boundaries [1].

For mapping the chemical information at these positions, ToF-SIMS was employed. In [5], an EBIC image of the degraded area was overlaid with a laterally resolved reconstruction of the measured Na intensity near the SiN/Si interface. It was shown that Na accumulates at positions that coincide well with PID-s-affected areas. Additionally, a significant increase of the Na signal was clearly visible at the SiN/Si interface.

In order to localize defects within the Si material and to discuss the increased recombination, cross sections have been prepared toward the shunt position by FIB as shown in detail elsewhere [16]. Here, only the main results shall be summarized to conclude the paper. The EBIC image of the FIB cross section in Fig. 6 reveals a well-defined p-n junction that is weakened substantially over a length of $\sim$10 μm at this PID-s-affected site. Below the location of the weakened p-n junction, a region which is located 0–4 μm below the emitter region shows a drastically reduced EBIC signal. In addition, a darker line indicates a line of defects within the area. These observations can be explained by a plane-like defect, which is lying in the [1 1 1] plane [15]. In Fig. 6, the geometrical situation at the FIB cross section of this defect is visualized. The red line indicates the puncture point of the defect in the cross section. Note that the cross section is not perfectly parallel to the base of the pyramidal structures.

In order to investigate structural properties and elemental composition of individual PID shunts on a nanometer scale, TEM experiments, including elemental analyses (EDX), have been performed in [16]. A FIB-lamella has been prepared at this position for TEM analysis. The TEM imaging at the lamella in Fig. 6 (right) shows a tilted defect line (a crystal defect) which is lying mainly in the depletion region. The crystal defect is assigned to a stacking fault lying in the [1 1 1] plane, which has been shown previously [9], [11]. Cross sections at nine different PID-s-affected sites have all revealed stacking faults in $\{1\,1\,1\}$ planes. In the following, the main results of the EDX measurements in STEM mode will be summarized in order to discuss the observed results. The SiN layer is indicated by a high EDX signal for N (yellow color in Fig. 6). An interlayer that contains O is clearly detected in the SiN/Si interface region (not shown here). The most important result is that the stacking fault is clearly decorated by Na impurities visualized in green in the TEM analysis in Fig. 6. In addition, Na is also detected in the SiO_x interlayer, where the stacking fault touches the interface.

VI. Discussion

Based on our results, the following facts can be claimed as partly done in [5] and [15]: 1) PID-s is influencing the parallel resistance (R_p) and the recombination behavior $(J_{02}$ and $n_2)$ of the solar cell. 2) The PID-s effect is not affecting the whole area but only single microscopic areas. [5], [15]. 3) At PID-s-affected areas, Na atoms have always been detected [5], [15]. 4) PID-s-affected sites always show modified stacking faults decorated with Na atoms which touch the surface [5], [15].

The stacking faults are considered to be present prior to degradation. However, they appear to accumulate Na during PID. In this contribution, the dynamics of Na movement through the SiN layer and at the interfaces or even at the stacking faults will not be discussed. For this discussion, see [11] and [17]. In this contribution, only the shunting and, in particular, the recombination processes will be discussed.

In [16], it is shown that quantitative evaluations of the EDX data for Si and Na reveal an areal density of Na atoms of approximately 6×10^{14} cm^{-2} in the stacking fault plane. Therefore, we assume a density of Na within the stacking fault in an order of magnitude that corresponds to one Si monolayer. In our case, Na atoms should be constrained to the stacking fault plane, probably located on interstitial sites. Since, in metallic Na, the Fermi level is lying in a continuum of states, it can be assumed that

the Na atoms lead to a band of gap states at multiple energies within the Si band gap, as sketched in Fig. 7. The blue-dashed arrow in Fig. 7 visualizes a path along the stacking fault, starting from the SiN/Si interface through the emitter across the p-n junction into the base where Na can travel. Here, it depends on the local defect level concentration and how this defect acts electronically.

If the local defect level concentration in the PID-s-affected area is very high, the defect orbitals of neighbored levels overlap, enabling hopping conduction for charge carriers under forward and reverse bias. Then, the monolayer acts like a quasi-metallic Na plane. This process needs no thermal activation and, therefore, leads to an ohmic conductivity across the p-n junction. Therefore, process 1 in Fig. 7 would explain the detrimental decrease of the parallel resistance R_p.

In addition to this, under injection conditions these defect levels will offer recombination paths for interlevel recombination of the electrons and holes in the depletion region (process 2 in Fig. 7). This process can occur already at a relatively low concentration level, where lateral hopping conduction has yet to occur. Process 2 is thermally activated and should lead to an increased J_{02} with an ideality factor n_2 larger than 2, as described by Steingrube *et al.* [12], because the density of defects is still sufficiently high such that recombination does not occur via isolated defect states, but rather occurs via coupled defect states. Additionally, it was shown in Fig. 6 that the stacking fault which is only about 3 μm in length is crossing the depletion region. Hence, the fact that the decorated stacking fault is mainly influencing the recombination behavior in the depletion region coincides well with our experimental results. In Section IV, an increased J_{02} and an ideality factor larger than 2 was clearly observed by LIT and single dark *I–V* curve measurements. The charge carriers in Fig. 7 are generated by illumination (light gray in Fig. 7) as minority carriers and recombine via the defect states within the depletion region. However, the measurements in this paper were done under electrical injection. Nevertheless, the physical recombination process is assumed to be identical.

VII. Summary

In this paper, we have introduced a PID test for solar-cell level and module components that is applicable as a tool for process control in industries and for root cause analysis in the laboratory. In addition, an analysis of a solar cell that is degraded by the PID tester is performed. It is shown that PID of the shunting type is influencing both the parallel resistance (R_p) and the depletion region recombination behavior (J_{02}) of the solar cell. The increased recombination in the depletion region is caused by Na-decorated stacking fault crossing the depletion region and, hence, influencing the recombination behavior of the depletion region strongly, reflected by an increased J_{02} and n_2 larger than 2. Since the stacking fault ends only a few micrometers below the surface, the base of the solar cell is primarily unaffected; hence, the J_{01} recombination is not increased. Based on these results, a model explaining the influence of PID-s on the shunting, as well as on the recombination behavior of the solar cell, was discussed. In particular, the increased J_{02} recombination is explained by an interlevel recombination of the electrons and holes in the depletion region at defect states caused by the Na-decorated stacking fault.

References

[1] S. Pingel, O. Frank, M. Winkler, S. Daryan, T. Geipel, H. Hoehne, and J. Berghold, "Potential induced degradation of solar cells and panels," in *Proc. 35th IEEE Photovoltaic Spec. Conf.*, Honolulu, HI, USA, 2010, pp. 002817–002822.

[2] J. Berghold, O. Frank, H. Hoehne, S. Pingel, B. Richardson, and M. Winkler, "Potential induced degradation of solar cells and panels," in *Proc. 25th Eur. Photovoltaic Sol. Energy Conf. Exhib.*, Valencia, Spain, 2010, pp. 3753–3759.

[3] P. Hacke, K. Terwilliger, R. Smith, S. Glick, J. Pankow, M. Kempe, S. Bennett, and M.o. Kloos, "System voltage potential-induced degradation mechanisms in PV modules and methods for test," in *Proc. 37th IEEE Photovoltaic Spec. Conf.*, Seattle, WA, USA, 2011, pp. 814–820.

[4] H. Nagel, A. Metz, and K. Wangemann, "Crystalline Si solar cells and modules featuring excellent stability against potential-induced degradation," in *Proc. 26th Eur. Photovoltaic Sol. Energy Conf. Exhib.*, Hamburg, Germany, 2011, pp. 3107–3112.

[5] V. Naumann, D. Lausch, A. Hähnel, J. Bauer, O. Breitenstein, A. Graff, M. Werner, S. Swatek, S. Großer, J. Bagdahn, and C. Hagendorf, "Explanation of potential-induced degradation of the shunting type by Na decoration of stacking faults in Si solar cells," *Sol. Energy Mater. Sol. Cells*, vol. 120, pp. 383–389, 2013.

[6] C. Taubitz, M. Schütze, and M. B. Köntopp, "Towards a kinetic model of potential-induced shunting," in *Proc. 27th Eur. Photovoltaic Sol. Energy Conf. Exhib.*, 2012, pp. 3172–3176.

[7] S. Koch, C. Seidel, P. Grunow, S. Krauter, and M. Schoppa, "Polarization effects and tests for crystalline silicon cells," presented at the 26th Eur. Photovoltaic Solar Energy Conf. Exhib., Hamburg, Germany, 2011.

[8] M. Schütze, M. Junghänel, O. Friedrichs, R. Wichtendahl, M. Scherff, J. Müller, and P. Wawer, "Investigations of potential induced degradation of silicon photovoltaic modules," presented at the 26th Eur. Photovoltaic Solar Energy Conf. Exhib., Hamburg, Germany, 2011.

[9] B. Otwin and M. Langenkamp, *Lock-In Thermography: Basics and Use for Functional Diagnostics of Electronic Components*. vol. 10, New York, NY, USA: Springer, 2003.

[10] J. Bauer, V. Naumann, S. Großer, C. Hagendorf, M. Schütze, and O. Breitenstein, "On the mechanism of potential-induced degradation in crystalline silicon solar cells," *Phys. Status Solidi*, vol. 6, no. 8, pp. 331–333, 2012.

[11] O. Breitenstein, "Nondestructive local analysis of current–voltage characteristics of solar cells by lock-in thermography," *Sol. Energy Mater. Sol. Cells*, vol. 95, pp. 2933–2936, 2011.

[12] S. Steingrube, O. Breitenstein, K. Ramspeck, S. Glunz, A. Schenk, and P. Altermatt, "Explanation of commonly observed shunt currents in c-Si solar cells by means of recombination statistics beyond the Shockley–Read–Hall approximation," *J. Appl. Phys.*, vol. 110, pp. 014515-1–014515-10, 2011.

[13] D. Lausch, K. Petter, R. Bakowskie, J. Bauer, O. Breitenstein, and C. Hagendorf, "Classification and investigation of recombination-active defect structures in multicrystalline silicon solar cells," in *Proc. 27th Eur. Photovoltaic Solar Energy Conf. Exhib.*, Frankfurt, Germany, 2012, pp. 723–728.

[14] H. Seidel, L. Csepregi, A. Heuberger, and H. Baumgärtel, "Anisotropic etching of crystalline silicon in alkaline solutions," *J. Electrochem. Soc.*, vol. 137, no. 11, pp. 3612–3626, 1990.

[15] V. Naumann, "Microstructural analysis of crystal defects leading to potential-induced degradation (PID) of Si solar cells," *Energy Procedia*, vol. 33, pp. 76–83, 2013.

[16] V. Naumann, D. Lausch, A. Graff, M. Werner, S. Swatek, J. Bauer, A. Hähnel, O. Breitenstein, S. Großer, J. Bagdahn, and C. Hagendorf, "The role of stacking faults for the formation of shunts during potential-induced degradation of crystalline Si solar cells," *Phys. Status Solidi*, vol. 7, no. 5, pp. 315–318, 2013.

[17] M. Schütze, M. Junghanel, M. B. Koentopp, S. Cwikla, S. Friedrich, J. W. Muller, and P. Wawer, "Laboratory study of potential induced degradation of silicon photovoltaic modules," in *Proc. 37th IEEE Photovoltaic Spec. Conf.*, Seattle, WA, USA, 2011, pp. 821–826.

Dominik Lausch received the diploma degree in physics from the University of Leipzig, Leipzig, Germany, in 2009. During his studies, he was with the company Q-Cells SE on various subjects, including his diploma thesis about the pre-breakdown luminescence of silicon solar cells. In 2012, he received the Ph.D. degree in natural science from the University of Halle, Halle, Germany, in cooperation with the Fraunhofer Center for Silicon Photovoltaics CSP, Halle, and Q-Cells SE, Thalheim, Germany. His dissertation explored the subject of the "*Influence of recombination active defects on the electrical properties of recombination active defects in silicon solar cells*," which received the PVSEC Student Award in 2012.

He is now a postdoctoral researcher with the Fraunhofer Center for Silicon Photovoltaics CSP, where he is currently dealing with plasma texturing and hydrogen passivation topics.

Volker Naumann received the degree in physics from the Martin-Luther-University Halle-Wittenberg, Germany, in Electric properties and microstructure of local contacts on silicon solar cells, in 2009. Currently, he is a young researcher and is pursuing the Ph.D. degree with the Fraunhofer Center for Silicon Photovoltaics CSP (Halle) and Martin-Luther-University Halle-Wittenberg, working on electrical and microstructure characterization of photovoltaic materials and processes.

He is particularly focussed on microstructural diagnostics and elemental analyses of antireflective layers with respect to PID shunting phenomena of crystalline Si-solar cells.

Otwin Breitenstein received the Ph.D. degree in physics from the University of Leipzig, Leipzig, Germany, in 1980.

Since 1992, he has been with the Max Planck Institute of Microstructure Physics, Halle, Germany, where he investigated defects in semiconductors. Since 1999, he has been using lock-in thermography for detecting internal shunts in silicon solar cells. In 2001, he introduced this technique on a microscopic scale for isolating faults in integrated circuits. He gives lectures on photovoltaics at Halle University and is author of a book on Lock-in Thermography. He has published more than 200 contributions in scientific journals and international conference proceedings.

Jan Bauer received the Diploma in physics from the University of Halle, Halle, Germany, in 2006, for an investigation on shunting precipitates in Si solar cell material, and the Ph.D. degree in solar cell characterization, particularly under reverse bias, from University of Halle in 2009, in cooperation with the Max Planck Institute of Microstructure Physics, Halle.

After being with CaliSolar Inc., Berlin, Germany, he is now a postdoctoral researcher with the Max Planck Institute of Microstructure Physics, Halle. His main research interest is the local loss analysis of solar cells and the microscopic investigation of defects limiting their efficiency.

Andreas Graff received the Diploma in physics from the RWTH Aachen, Aachen, Germany, in 1995 and the Ph.D. degree in physics from the University of Halle, Halle, Germany, in 1999 for the investigations of interface structures during solid-state reactions. The experiments were done at the Max Planck Institute for Microstructure Physics, Halle.

He then spent 3 years with the IFW Dresden, Dresden, Germany, where he worked with analytical transmission electron microscopy (TEM), mostly on carbon-based materials. He joined the Fraunhofer Institute of Mechanics of Materials, Halle, in 2004, where he has been investigating defects in semiconductor devices by analytical TEM with the Center for Applied Microstructure Diagnostics (CAM).

Christian Hagendorf received the Ph.D. degree from the Martin-Luther-University Halle-Wittenberg, Germany, in the field of surface and interface analysis of semiconductor materials.

He is head of the research group "Solar Cell Diagnostics" with the Fraunhofer Center for Silicon Photovoltaics CSP, Germany. He joined Fraunhofer CSP in 2007 and established a research group focussed on defect diagnostics in crystalline and thin-film photovoltaics. His research activities rely on electrical, microstructural, and trace elemental characterization of solar cells and modules.

Jörg Bagdahn received the diploma and the Ph.D. degrees in material science from the Technical University of Chemnitz and Martin-Luther-University, Halle, Germany, respectively.

From 2000 until 2002, he was a postdoctoral fellow with Johns Hopkins University, Baltimore, MD, USA, working on long-term reliability of thin silicon films. In 2003, he joined the Fraunhofer Institute for Mechanics of Materials, where he worked as a group leader and later on as head of the department "Microelectronics and Microsystems." Since 2007, he has been the director of the Fraunhofer Center for Silicon Photovoltaics CSP. Since 2008, he has held a professorship for "Photovoltaic Materials" with the Anhalt University of Applied Sciences.